some critical amplitude the vibration would become unstable. Although no quantitative data were obtained, it was observed that this critical amplitude (which was about 3 shell thicknesses for the $n = 10$ mode) depended on the circumferential wave number n. It is suspected that this is evidence of the occurrence of the companion mode instability observed in the ring vibrations.

Conclusions

The experimental results presented support the thesis that the nonlinear vibrations of thin cylindrical shells in mode shapes with long axial wavelengths exhibit many of the phenomena previously observed for thin circular rings. In particular, for amplitudes of the order of the shell thickness, the vibrations exhibit a slight nonlinearity of the "softening" type.

References

[1] Evensen, D. A., "Some observations on the nonlinear vibration of thin cylindrical shells," AIAA J. **1**, 2857–2858 (1963).

[2] Chu, H. N., "Influence of large amplitudes on flexural vibrations of a thin circular cylindrical shell," J. Aerospace Sci. **28**, 602–609 (1961).

[3] Nowinski, J., "Nonlinear transverse vibrations of orthotropic cylindrical shells," AIAA J. **1**, 617–620 (1963).

[4] Evensen, D. A., "Nonlinear flexural vibrations of thin circular rings," Ph.D. Thesis, California Institute of Technology (June 1964).

[5] Olson, M. D., "Supersonic flutter of circular cylindrical shells subjected to internal pressure and axial compression," Guggenheim Aeronautical Lab., California Institute of Technology Structural Dynamics Rept. SM 65-7, Air Force Office of Scientific Research 65-0599 (April 1965).

[6] Schmidt, L. V., "Measurements of fluctuating air loads on a circular cylinder," Ph.D. Thesis, California Institute of Technology (June 1963).

Electromagnetic Generation of High Dynamic Buckling Pressures

WOLFGANG A. KAPP* AND DONALD G. LEMKE†
Chrysler Corporation, Detroit, Mich.

Nomenclature

$\hat{H}$ = magnetic induction
n = number of turns per unit length
$f(x, y, R, l)$ = geometry function
R = radius of solenoid
x_p = coordinate along solenoid axis
l = length of solenoid
I_p = current in solenoid
C = discharge circuit capacity
Δ = width of search coil or specimen section
p = y/R
I_s = current in specimen
x = running coordinate along solenoid axis
y = running coordinate along solenoid radius
K = force
P = pressure
L = discharge circuit inductance
ρ_s = resistance of specimen
t = time
F = cross section of specimen
$k_1 = (2x_p + l)/2R$
$k_2 = (2x_p - l)/2R$

Presented as Preprint 64-486 at the 1st AIAA Annual Meeting, Washington, D. C., June 29–July 2, 1964; revision received June 14, 1965.

* Research Engineering Specialist; now Physicist, Advanced Theory Group, U.S. Air Force Flight Dynamics Laboratory, Wright Patterson Air Force Base, Ohio.

† Associate Scientist, Missile Division; now Assistant Professor of Engineering Mechanics, Michigan Technological University, Houghton, Mich.

Introduction

CURRENT defense concepts for protection against ballistic war heads call for employment of nuclear blast to aid in the destruction of the attacking re-entry vehicle. Hence, effort must be directed toward simulation of the associated phenomena in the laboratory.

Because of the high closure rate between the blast front and the re-entry vehicle, the pressure pulse applied to the re-entry vehicle structure can be expected to have a duration in the μsec range. Shell design criteria for pressure pulses of this type are based on studies[1] accomplished with pressure pulses in the millisecond range. There is reason to question the applicability of these criteria, since the pulse duration is too long to excite the shell ring mode.

Investigations[2,3] using conventional explosives all lack that one ingredient so necessary in experimental studies, i.e., control. In addition, conventional explosives introduce hazards and instrumentation difficulties, which are not to be overlooked.

Lindberg[4] utilizes very thin shells to demonstrate the interaction between the elastic extensional mode and the elastic flexural modes. The use of such thin shells was rejected by the authors because of the difficulty of eliminating imperfections caused by fabrication and also because the possible existence of a relationship between the ring mode and breathing mode frequencies might preclude use of such specimens.

Experimental Techniques

A metallic shell is inserted into a coil through which a high-energy capacitor bank is discharged. The circuit is critically damped to avoid ringing. This discharge gives rise to a magnetic field, which, in turn, induces a current in the specimen. The inducing and induced currents generate magnetic fields that repel each other, thus generating the pressure pulse. Since it is possible to calculate the magnetic fields, the pressure can be determined. Both radially symmetric and asymmetric pulses can be generated by the simple expedient of varying the radial location of the specimen within the coil. Presently, studies are being conducted for devising a pressure gage on photoelastic principles. Although results are encouraging, satisfactory measurements have not yet been obtained. Space limitations prevent further elaborations.

Analytical Development

In the following, an analytic expression for the pressure will be derived. Consider the force acting on a current I_s in a magnetic field $\hat{H}$. It may be calculated from

$$dK = \hat{H} I_s \, dl \sin(\hat{H}, dl) \tag{1}$$

In this case, only the axial component of the field is important, and $\sin(\hat{H}, dl)$ may be assumed to equal 1. For a cylindrical coil, $\hat{H}$ has been determined to be[7]

$$\hat{H}_{ax} = \frac{In}{R} \int_0^\pi \left[\frac{2x_p - l}{(1 + p^2 + k_2^2 - 2p\cos\gamma)^{1/2}} - \frac{2x_p + l}{(1 + p^2 + k_1^2 - 2p\cos\gamma)^{1/2}} \right] \frac{1 - p\cos\gamma}{(1 + p^2 - 2p\cos\gamma)} \, d\gamma \tag{2}$$

To determine I_s, we compute the mean induced voltage in a ring segment of the specimen of width Δ at the distance $x_p + \Delta/2$ from the origin:

$$E\left(x + \frac{\Delta}{2}, t\right) = -\frac{2n}{\Delta} \frac{dI_p}{dt} \int_x^{x+\Delta} \int_F f(x, y, R, l) dF dx \tag{3}$$

From (3), we obtain the current in the ring section as

$$I_s = -\frac{2n}{\Delta\rho s} \frac{dI_p}{dt} \int_x^{x+\Delta} \int_F f(x, y, R, l) \, dF dx \tag{4}$$

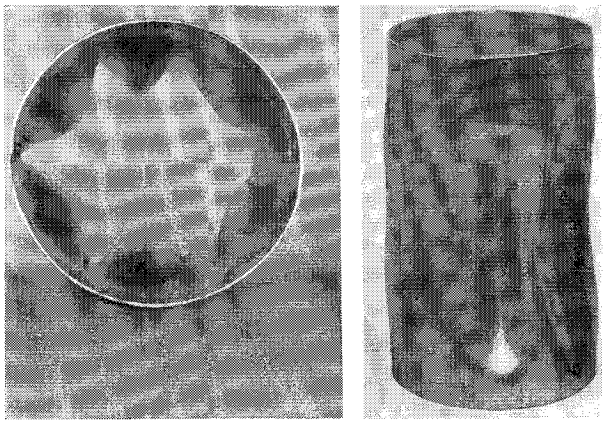

Fig. 1 Buckled shell specimen, symmetric case.

Thus, the total pressure on a ring element of length dl and width Δ at a distance $x + \Delta/2$ from the origin will be

$$P = -\frac{2nI_p}{\Delta} f(x, y, R, l) \cdot \frac{2n}{\Delta\rho s} \frac{dI_p}{dt} \cdot \int_x^{x+\Delta} \int_F f(x, y, R, l) dx dF \tag{5}$$

I_s can only be determined approximately, since $f(x, y, R, l)$ cannot be represented in closed form. To overcome this difficulty, an experimental method of measuring I_s directly has been devised.

The specimen current is determined by means of a search coil, which is placed in the proper position inside the buckling coil. It consists of a circular metal loop whose diameter and thickness are equal to those of the specimen. This is necessary in order to avoid errors. The width is equal to the integration interval or ring section width in Eqs. (4) and (5). The loop is prevented from buckling by a phenolic insert. The signal from this coil is fed into an oscilloscope, which records amplitude, time dependence, and phase of the search coil current.

Thus, the final equation for the pressure may be written as

$$P = -(2nI_p/\Delta) I_s f(x, y, R, l) \tag{6}$$

Except for the geometry function f, this equation contains only directly measurable variables. The function f, however, is easily computed and tabulated. Furthermore, note that f represents the total geometric input to the calculation so that the total pressure anywhere in the coil can be obtained. The time dependence of this pressure is determined by the time dependencies of I_p and I_s that can be established by measurement.

Illustrative Example

To demonstrate the calculation in an expository fashion we must choose a simple example that eliminates the numerical integration. This requires that various simplifying assumptions be made. Consider the case of a cylindrical specimen centrally located in a cylindrical coil. For simplicity, the field is assumed uniform over the cross section of the solenoid and equal to its value on the axis. Modifying Eq. (2) for the assumed conditions yields

$$\hat{H} = 2\, nI_p f(x, y, R, l) = 2\pi nI \left\{ \frac{2x + l}{[4R^2 + (2x + l)^2]^{1/2}} - \frac{2x - l}{[4R^2 + (2x - l)^2]^{1/2}} \right\} \tag{7}$$

Assume $I_p = I_{p\,\max} \sin\omega t$ for the leading edge of I_p. Hence, one receives from Eqs. (2) and (3), after some algebraic manipulation, integration over the circumference of the specimen and division by the surface area:

$$P = -(2\pi^3 n^2 R^2 \omega / l\rho_s) I_{p\,\max}{}^2 \sin 2\omega t\, f^2(x, y, l, R) \tag{8}$$

This expression, however, is applicable only as long as no deformation of the specimen has taken place. By including the discharge circuit parameters, Eq. (8) reduces to

$$P = -(0.1\pi I_{p\,\max}{}^2 / 2\rho_s l)(L/C)^{1/2} f^2(x, y, R, l) \sin 2\omega t \tag{9}$$

where $[P]$ = dynes cm^{-2}, $[\rho_s]$ = ohms, $[C]$ = farads, $[I]$ = amperes, and $[L]$ = henries.

Let us now assume a cylinder 40 cm long and 8 cm in diameter with $\rho_s \approx 10^{-2}$ ohms. Let the circuit constants be $L = 10^{-4}$ H_y, $C = 500$ μfarads, and $I_p = 10^4$ amp. Inserting these values into Eq. (9) yields a maximum pressure of 6.6×10^7 dynes cm^{-2} or approximately 920 psi.

Experimental Results

Copper, aluminum, and stainless-steel specimens requiring static buckling pressures of over 600 psi have been buckled by this method. Changes in the buckling mode have been noted between the static and dynamic cases. For example, Fig. 1 shows the dynamic buckling results obtained for a typical symmetric loading dynamically applied in 25 μsec. Sturm[5] predicted that this specimen should buckle under static loading at 605 psi with four nodes. The important result is that the shell buckled with six nodes rather than the expected four nodes. This disagreement clearly indicates an interaction between vibration and buckling. The dynamic buckling result obtained for a typical asymmetric loading is shown in Fig. 2. The electrical energy input for generating the pulse was the same as for the specimen shown in Fig. 1. The only basic difference was locating the specimen eccentrically in the test coil. One need only consider the difficulty of duplicating this loading by other means and under controlled pulse-time conditions to realize the significance of this result. From the experimental results obtained, it can be concluded that this technique fulfills the requirements established regarding the pressure-time relation necessary to excite the shell ring mode. In addition, it permits the use of actual hardware materials and thus an extension into post yield response. By coupling the capability of this technique with the modeling laws outlined by Baker et al.,[6] the authors feel that a great deal can be accomplished in the area of blast loading of the type discussed, as well as longer-duration loadings.

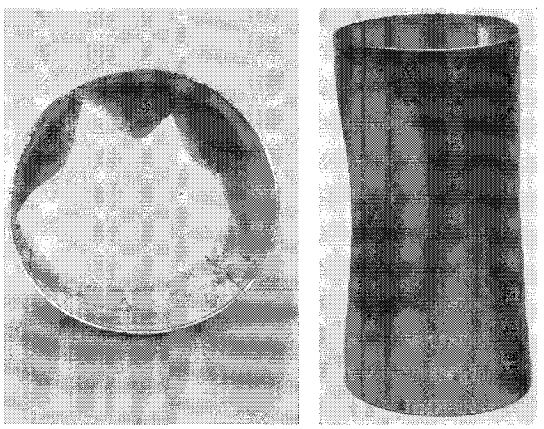

Fig. 2 Buckled shell specimen, asymmetric case.

References

[1] Barton, M. V. et al., "Final report on buckling of shells under dynamic loads," Space Technology Labs., Inc., TR 8622-0001-RV-000 (October 1961).

[2] Abrahamson, G. R., "Investigation of response of simplified ICBM-type structures, Vol. II," Tech. Doc. Rept. AFSW-TDR-62-94, Air Force Special Weapons Center, Air Force Systems Command, Kirtland Air Force Base, N. Mex. (December 1962).

[3] DeHart, R. C. and Basdekas, N. L., "Response of aircraft fuselages and missile bodies to blast loading," Tech. Doc. Rept. ASD-TDR-62-Y58, Flight Dynamics Lab., Aeronautical Systems

Div., Air Force Systems Command, Wright-Patterson Air Force Base, Ohio (January 1963).

[4] Lindberg, H. E., "Buckling of a very thin cylindrical shell due to an impulsive pressure," American Society of Mechanical Engineers Paper 63-APMW-7 (1963).

[5] Sturm, R. G., "A study of the collapsing pressure of thin-walled cylinders," Engineering Experiment Station, Univ. of Illinois Bull. 329 (1941).

[6] Baker, W. E., Ewing, W. O., and Hanna, J. W., "Laws for large elastic response and permanent deformation of model structures subjected to blast loading," Ballistic Research Laboratories, Aberdeen Proving Ground, Md. Rept. 1060 (December 1958).

[7] Kapp, W. A. and Lemke, D. G., "Electromagnetic generation of high dynamic buckling pressures," AIAA Preprint 64-486 (1964); reader is warned of errors in Eq. (B1).

Large Deflections of Thin Rods under Nonsymmetric Distributed Loads

TEH HWEI LEE*
The Boeing Company, Seattle, Wash.

Introduction

THE analytic approximate solution to nonlinear bending problems of elastic rods under distributed loads has been supplied by Christensen[1] using the Ritz method with one term of a trigonometric series. Such single-term solutions can no longer give a satisfactory approximation when nonsymmetric loads are present. As a remedy, a two-term solution is presented in this note.

Two-Term Galerkin Solution

The governing differential equation for the system shown in Fig. 1 has the form

$$d/ds[EI(d\theta/ds)] - H\sin\theta + V\cos\theta = 0 \qquad (1)$$

where

$$H = H_0 + \int_0^s p(s)\,ds = H_l - \int_s^l p(s)\,ds$$

$$V = V_0 - \int_0^s q(s)\,ds = \int_s^l q(s)\,ds - V_l$$

The approximate solution of Eq. (1) is assumed to be

$$\tilde{\theta} = \theta_1\cos\beta s + \theta_2\cos 2\beta s \qquad \beta = \pi/l \qquad (2)$$

Then, by Galerkin's method,[2] the constants θ_1 and θ_2 are determined by the system of equations

$$\int_0^l NL(\tilde{\theta})\cos\beta s\,ds = 0 \qquad \int_0^l NL(\tilde{\theta})\cos 2\beta s\,ds = 0 \qquad (3)$$

and $NL(\theta)$ represents the nonlinear differential equation (1).

The integration in (3) can be carried out by making use of the trigonometric identities and the expansions of Bessel series.[3] It can be shown that, for a thin rod with a constant flexural rigidity EI under uniformly distributed loads of intensities p_0 and q_0, Eqs. (3), upon integration, lead to the following simultaneous transcendental equations:

$$\left.\begin{aligned} &\theta_1 P_c/Q_0 + (2H_0/Q_0 + m)A_1 + mB_1 + \\ &\qquad (2V_0/Q_0 - 1)C_1 - D_1 = 0 \\ &4\theta_2 P_c/Q_0 + (2H_0/Q_0 + m)A_2 + mB_2 + \\ &\qquad (2V_0/Q_0 - 1)C_2 + D_2 = 0 \\ &\qquad (Q_0 \neq 0) \end{aligned}\right\} \qquad (4)$$

Received May 13, 1965.

* Associate Research Engineer.

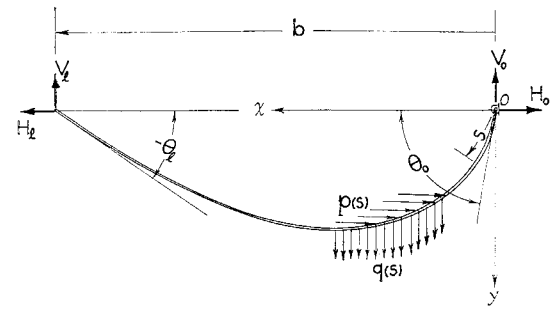

Fig. 1 Simply supported elastic thin rod loaded nonsymmetrically.

where the symbols are defined as follows:

$$P_c = \pi^2 EI/l^2 \qquad Q_0 = q_0 l \qquad m = p_0/q_0$$

$$A_1 = J_1(\theta_1)J_0(\theta_2) + \sum_{k=1}^{\infty}(-1)^k J_{2k}(\theta_2)[J_{4k+1}(\theta_1) - J_{4k-1}(\theta_1)]$$

$$B_1 = \left(\frac{8}{\pi^2}\right)\left\{\sum_{k=1}^{\infty}(-1)^k J_0(\theta_1)J_{2k-1}(\theta_2)\times \frac{(4k-2)^2+1}{[(4k-2)^2-1]^2} + \sum_{j=1}^{\infty}\sum_{k=1}^{\infty}(-1)^{j+k}J_{2j}(\theta_1)J_{2k-1}(\theta_2)\times \left[\frac{c_1^2+1}{(c_1^2-1)^2} + \frac{c_2^2+1}{(c_2^2-1)^2}\right]\right\}$$

$$c_1 = 4k + 2j - 2 \qquad c_2 = 4k - 2j - 2$$

$$C_1 = \sum_{k=1}^{\infty}(-1)^k J_{2k-1}(\theta_2)[J_{4k-1}(\theta_1) - J_{4k-3}(\theta_1)]$$

$$D_1 = \left(\frac{8}{\pi^2}\right)\left\{\frac{J_0(\theta_2)J_0(\theta_1)}{2} + \sum_{k=1}^{\infty}(-1)^k \times \left[\frac{J_0(\theta_2)J_{2k}(\theta_1)(4k^2+1)}{(4k^2-1)^2} + \frac{J_0(\theta_1)J_{2k}(\theta_2)(16k^2+1)}{(16k^2-1)^2}\right] + \sum_{j=1}^{\infty}\sum_{k=1}^{\infty}(-1)^{j+k}J_{2j}(\theta_1)J_{2k}(\theta_2)\times\left[\frac{c_3^2+1}{(c_3^2-1)^2} + \frac{c_4^2+1}{(c_4^2-1)^2}\right]\right\}$$

$$c_3 = 4k + 2j \qquad c_4 = 4k - 2j$$

$$A_2 = J_0(\theta_1)J_1(\theta_2) - \sum_{k=1}^{\infty}(-1)^k J_{2k-1}(\theta_2)[J_{4k-4}(\theta_1) + J_{4k}(\theta_1)]$$

$$B_2 = \left(\frac{8}{\pi^2}\right)\left\{\sum_{k=1}^{\infty}(-1)^k J_0(\theta_2)J_{2k-1}(\theta_1)\left[\frac{(2k-1)^2+4}{[(2k-1)^2-4]^2}\right] + \sum_{j=1}^{\infty}\sum_{k=1}^{\infty}(-1)^{j+k}\times J_{2j-1}(\theta_1)J_{2k}(\theta_2)\times\left[\frac{c_5^2+4}{(c_5^2-4)^2} + \frac{c_6^2+4}{(c_6^2-4)^2}\right]\right\}$$

$$c_5 = 4k + 2j - 1 \qquad c_6 = 4k - 2j + 1$$

$$C_2 = J_0(\theta_2)J_2(\theta_1) + \sum_{k=1}^{\infty}(-1)^k J_{2k}(\theta_2)[J_{4k+2}(\theta_1) + J_{4k-2}(\theta_1)]$$

$$D_2 = \frac{8}{\pi^2}\sum_{j=1}^{\infty}\sum_{k=1}^{\infty}(-1)^{j+k}J_{2j-1}(\theta_1)J_{2k-1}(\theta_2)\times\left[\frac{c_7^2+4}{(c_7^2-4)^2} + \frac{c_8^2+4}{(c_8^2-4)^2}\right]$$

$$c_7 = 4k + 2j - 3 \qquad c_8 = 4k - 2j - 1$$

In Eqs. (4), the force V_0 is not an independent quantity. It is related to the external loads by the condition of equilibrium. Summing moments about the left end point yields

$$V_0 b - \int_0^l q_0(b-x)ds + \int_0^l p_0 y\,ds = V_0 b - q_0 bl + q_0\int_0^l\left[\int_0^s \cos\tilde{\theta}\,ds\right]ds + p_0\int_0^l\left[\int_0^s \sin\tilde{\theta}\,ds\right]ds = 0 \qquad (5)$$